arXiv:1611.08420v1 [cs.IT] 25 Nov 2016

Demonstration of Fully Nonlinear Spectrum Modulated System in the Highly Nonlinear Optical Transmission Regime

Vahid Aref, Son T. Le, and Henning Buelow

Nokia Bell Labs, Lorenzstr. 10, 70435 Stuttgart, Germany, firstname.lastname@nokia-bell-labs.com

Abstract *We report a 3 dB increase in the nonlinear threshold of a 64 $\times$ 0.5Gbaud 16-QAM continuous-nonlinear-spectrum modulated signal by nonlinear multiplexing with QPSK modulated multi-solitons, showing the first ever fully nonlinear-spectrum modulated system in the highly nonlinear regime.*

Introduction

Recent advances in coherent technology and applying digital signal processing techniques, originally developed for classical linear channels, enable us to achieve the spectral efficiency (SE) close to the "presumed" upper-bound of AWGN capacity for low power signals in which the channel is fairly linear. However, the achievable SE decreases for launch powers beyond some "nonlinear threshold" as the channel becomes very nonlinear. The nonlinear threshold depends on modulation formats, pulse-shaping, and can be improved by more complex equalization techniques such as digital back propagation.

Nonlinear Fourier transform (NFT) characterizes the complex signal propagation in optical fiber by some simple evolution rules. It maps each pulse in a nonlinear spectrum, partitioned to continuous and discrete part. Continuous spectrum represents the "dispersive" part of the pulse while the discrete spectrum represents the "solitonic" part, nonlinearly multiplexed to the dispersive part. Solitonic part appears when the pulse has a large power.

As a pulse propagates in a lossless-noiseless fiber, the modes of nonlinear spectrum are independently evolved. This fact proposes to modulate data over these modes. Accordingly, the modulation of OFDM symbols in the continuous spectrum is demonstrated in [1] showing the potential performance gain over the classical OFDM symbols. However, the performance still degrades by increasing power beyond some nonlinear threshold. Moreover, modulation of pure solitonic pulses (without continuous part) is demonstrated in [2], [3], [4]. However, the achieved SE is so far very low, and multi-solitons are observed susceptible to imperfect transmission conditions.

In this paper, we demonstrate for the first time the modulation over both discrete and continuous parts by developing a low-complexity inverse NFT (INFT) algorithm. On the continuous spectrum, we modulate 64×0.5 Gbaud OFDM signals with 16-QAM format and on the discrete spectrum, we consider a hybrid modulation of eigenvalues and spectral amplitudes: First two eigenvalues are chosen out of a set of eigenvalues and then, the spectral amplitude of each chosen eigenvalue is QPSK modulated. These two QPSK modulated solitons, carrying additional few information bits, are multiplexed with the signal of continuous part.

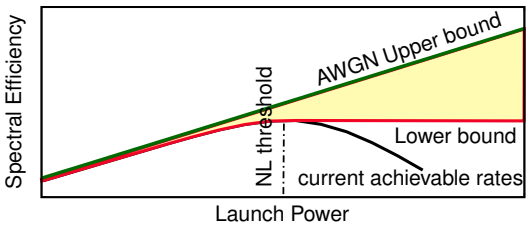

Fig. 1: The spectral efficiency of a typical coherent optical system.

We demonstrate the transmission over 18×81.3 km in a SMF fiber loop with EDFAs. The signal of each spectrum are detected independently in nonlinear spectrum. We show that the nonlinear threshold will be increased proportional to the additional power in discrete spectrum. However, the performance of continuous spectrum is slightly degraded by multiplexing multi-solitons. This can be because of larger pick-to-average power ratio, and more importantly, the weak correlation between two spectra caused by the noise of amplifiers and by the lumped amplification.

Modulation of Discrete and Continuous Spectrum

The nonlinear spectrum of a pulse $q(t)$ has two parts: The continuous part, denoted by $q_c(\lambda)$, is the spectral amplitudes for real valued frequencies $\lambda \in \mathbb{R}$. The discrete part contains a finite set of complex eigenvalues $\{\lambda_k\} \subset \mathbb{C}^+$ and the corresponding spectral amplitudes $q_d(\lambda_k)$. The spectral amplitudes are defined based on Zakharov-Shabat system. We refer the reader to [5] for detailed definitions and properties. We modulate information bits over both spectrum as follows:

A. Continuous Spectrum: We modulate 256 bits over $N = 64$ overlapping orthogonal subchannels in the continuous spectrum in a similar way as the

conventional OFDM signal is designed in the linear Fourier spectrum. For each symbol, the continuous spectrum was defined as:

$$q_c(\omega) = A\sum_{k=-N/2}^{N/2} C_k \mathrm{sinc}(\tfrac{T_c}{\pi}\omega + k), \omega \in \mathbb{R}, \quad (1)$$

where C_k is drawn from 16-QAM constellation, A is the power control parameter, $T_c = 2$ ns is the useful block duration defining the baud-rate of 0.5Gbaud. To avoid ISI during propagation, we consider two guard intervals of 4 ns, resulting the total symbol duration $T_s = 10$ ns and the raw data rate of 25.6 Gb/s modulated in continuous part.

B. Discrete Spectrum: We modulate the position of two purely imaginary eigenvalues λ_1 and λ_2 in the upper complex plane as well as the phase of their spectral amplitudes. Each circle in Fig. 5 (a) illustrates a pair of the 12 possible (λ_1, λ_2) which are used for modulation. In addition, the phase of each spectral amplitude, $\triangleleft q_d(\lambda_k)$, is independently modulated with a QPSK constellation, as shown in Fig. 5 (b). Determining the temporal position of each "sech" shape in the symbol (see Fig. 2), $|q_d(\lambda_k)|$ are chosen such that a "sech" shape occurs every almost 5 ns in the block of symbols. We denote this modulation by $D2$.

We also consider another modulation scheme, denoted here by $D1$, with the different eigenvalue set of $\{1j, 1.5j\}$. One bit is thus modulated by two possible pairs of (λ_1, λ_2). The spectral amplitudes are modulated similar to $D2$. The average power of discrete spectrum for each of modulations is,

$$\begin{aligned} P_{\mathrm{d}} &= \tfrac{|\beta_2|}{\gamma T_0^2} \approx 0.016 \text{ mW, for } D1 \\ P_{\mathrm{d}} &= 2\tfrac{|\beta_2|}{\gamma T_0^2} \approx 0.032 \text{ mW, for } D2 \end{aligned} \quad (2)$$

for $\beta_2 = -21.3\ \frac{\mathrm{ps}^2}{km}$, $\gamma = 1.3 \frac{\mathrm{W}^{-1}}{\mathrm{km}}$, and scaling factor $T_0 = 1$ ns.

Moreover, 5 bits are modulated per symbol in $D1$ and $4 + \log_2(12)$ bits in $D2$, resulting the rate of 0.5Gb/s and 0.76 Gb/s, respectively.

C. Multiplexing Spectrum: To multiplex both spectrum, denoted by $(C \boxplus D)$, we extend the Darboux transformation used to generate a multi-soliton pulse. It initially starts with $q(t) = 0$ and updates $q(t)$ by adding eigenvalue one-by-one. The algorithm and how nonlinear spectrum is changed by updating $q(t)$ are described in [6]. We apply the Darboux transformation with initial pulse $q(t) = \tilde{q}(t) \neq 0$. To add the eigenvalue λ_k, we need a solution of Zakharov-Shabat system at this spectral parameter λ_k. For the sake of space, we skip here how one can find a suitable solution. Having this solution, we can update $q(t)$ to a pulse having eigenvalue λ_k. According to [6, Theorem 1], the continuous spectrum of the pulse after adding n eigenvalues $\{\lambda_1, \ldots, \lambda_n\}$ is,

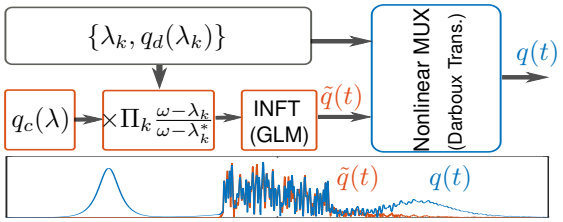

Fig. 2: Multiplexing discrete and continuous spectrum

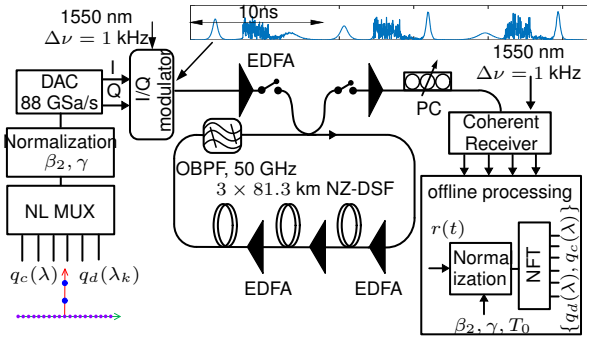

Fig. 3: Experimental setup with offline NFT-based detection

$$q_c(\omega) = \tilde{q}_c(\omega) \prod_{k=1}^{n} \tfrac{\omega-\lambda_k^*}{\omega-\lambda_k}, \quad (3)$$

where $\tilde{q}_c(\omega)$ denotes the continuous spectrum of the initial pulse $\tilde{q}(t)$. To have the given $q_c(\omega)$ in Eq. 1, we first apply the inverse of evolution Eq. 3. For taking inverse NFT, we then use the Gelfand-Levitan-Marchenko (GLM) algorithm [1] to find $\tilde{q}(t)$ and finally apply the Darboux transformation. The diagram of the algorithm including a pulse of $(C \boxplus D2)$ are shown in Fig. 2.

Experimental results

The experimental setup with a re-circulating loop is illustrated in Fig. 3. The time domain signal $q(t)$ was generated from multiplexing symbol by symbol random streams of continuous and discrete spectrum having the total power, $P = P_{\mathrm{d}} + P_{\mathrm{c}}$ where P_{d} is fixed as Eq. 2, and P_{c} is controlled by parameter A in Eq. 1. After resampling to 88 GSa/s, $q(t)$ is normalized according to the path averaged model of links with lumped amplifiers.

The fiber loop consists of 3×81.3 km spans of standard single mode fiber and EDFAs. Both the transmitter laser and local oscillator were from a single fiber laser source with 1 kHz linewidth. At the receiver, after coherent detection, digital sampling at 80 GSa/s, timing synchronization and frequency offset compensation; the received signal was normalized to the initial power P. Next, for each 10 ns symbol, NFT was applied separately on each spectrum as follows:

A. Continuous Spectrum: The detection of 64×0.5GBaud 16-QAM OFDM symbols were carried

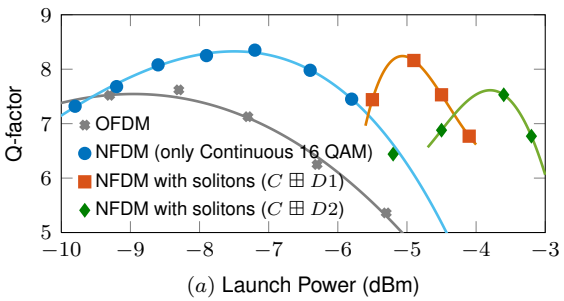

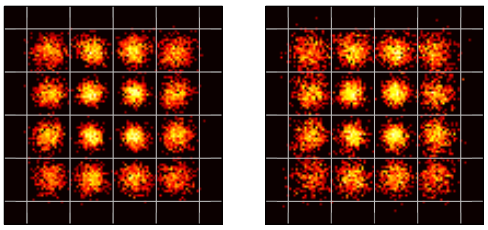

(b) 16−QAM of $(C \boxplus D1)$ (c) 16-QAM of $(C \boxplus D2)$

Fig. 4: Continuous spectrum of received pulses: (a) Q-factor vs. P. 16− QAM constellation of received 64 subchannels for (b) $(C \boxplus D1)$ and (c) $(C \boxplus D2)$

out according to [1] in which single-tap phase-shift removal operation was performed to remove the interplay of dispersion and nonlinearity followed then by channel equalization and phase noise estimation. The transmission performance of 1460 km link is shown in Fig. 4 in terms of the Q-factor directly derived from the bit-error-rate (BER), where more than 100 errors were obtained for each calculated BER value. In all curves, the launch power is tuned by changing only the power of continuous spectrum, P_{c}.

In comparison to conventional 64×0.5GBaud 16-QAM OFDM, the NFDM (OFDM in continuous spectrum) shows about 0.7 dB gain in Q-factor with a larger nonlinear threshold. Multiplexing with discrete spectrum, the nonlinear threshold (of continuous part) is increased by about 2 dB for $(C \boxplus D1)$ and by about 3 dB for $(C \boxplus D2)$. These values are consistent with the additional P_{d} of $(D1)$ and $(D2)$. Almost no decrease in Q-factor for $(C \boxplus D1)$ indicates a low interference between the continuous and discrete spectrum in presence of noise and other perturbations from ideal fiber model. The performance degradation in $(C \boxplus D2)$ is mainly because of large peak-to-average-power-ratio and limited resolution of ADC in receiver. The solitons keep their large amplitudes but the dispersive part of the pulse (continuous spectrum) spreads out into the guard bands and its effective amplitude decreases. Thus, the dispersive part is captured with lower resolution than the case of without solitonic part.

B. Discrete Spectrum: The discrete spectrum of each symbol $\{(\hat{\lambda}_1, \hat{q}_d(\hat{\lambda}_1)), (\hat{\lambda}_2, \hat{q}_d(\hat{\lambda}_2))\}$ is computed via Forward-Backward NFT algorithm [6].

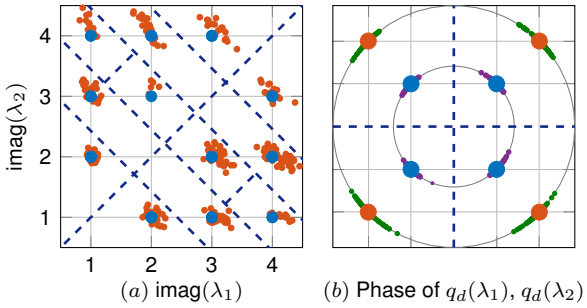

Fig. 5: Discrete spectrum of received pulses for $(C \boxplus D2)$: (a) imaginary part of received eigenvalues and (b) $\sphericalangle q_d(\lambda_k)$

After eigenvalues detection, the encoded phase is detected by the single-tap phase-shift removal operation performed according to designed eigenvalues [2], and applying the phase noise estimation derived for continuous part.

For $(C \boxplus D2)$, the discrete spectrum of 300 received symbols is shown in Fig. 5 transmitted at the nonlinear threshold. The two independent $q_d(\lambda_k)$ are depicted in the same plot. The dots represent the received spectrum, and the circles are the sent constellation points. The normalized error of eigenvalues

$$(e_1, e_2) = \tfrac{1}{\mathrm{imag}(\lambda_1+\lambda_2)}(\hat{\lambda}_1 - \lambda_1, \hat{\lambda}_2 - \lambda_2)$$

are correlated $corr(e_1, e_2) \approx -0.499 - 0.03j$ implying

$$\hat{\lambda}_1 + \hat{\lambda}_2 \approx (\lambda_1 + \lambda_2)(1 + \epsilon),$$

where ϵ is a small random variable with $\mathbb{E}(|\epsilon|^2) < 10^{-3}$. It suggests (i) the decision regions as shown by dashed line in Fig. 5 (a), and more importantly, (ii) there is a small power exchange between discrete and continuous spectrum. By fitting a Gaussian mixture model, the BER is estimated resulting Q-factor beyond 14 dB. A higher Q-factor is also estimated for both phases of $q_d(\hat{\lambda}_1)$ and $q_d(\hat{\lambda}_2)$ shown in Fig. 5 (b). Thus, the achievable rate is very close to the maximum $4 + \log_2(12)$ information bits (error-free channel).

Similar performance is observed for other launch powers and also for the case $(C \boxplus D1)$ indicating an almost error-free transmission.

Conclusions

For the first time, the modulation of both continuous spectrum and discrete spectrum was demonstrated in experiment. We observed that: (i) The continuous and discrete spectrum are “almost” uncorrelated. (ii) The nonlinear threshold of continuous spectrum increases by about the power of discrete spectrum. (iii) The large PAPR of the discrete part increases the quantization error of ADC which degrades the performance. (iv) Encoding more bits on discrete part seems quite feasible increasing the total SE.

References

[1] S. T. Le, *et al.*“ Nonlinear inverse synthesis technique for optical links with lumped amplification,” Optics express, 2015.

[2] V. Aref, *et al.*“ Experimental demonstration of nonlinear frequency division multiplexed transmission,” Proc. ECOC 2015, Tu.1.1.2

[3] Z. Dong, *et al.* “Nonlinear frequency division multiplexed transmissions based on nft,” IEEE PTL, no. 15, 2015.

[4] H. Buelow, *et al.* “Transmission of waveforms determined by 7 eigenvalues with psk-modulated spectral amplitudes,” Proc. ECOC, 2016.

[5] M. I. Yousefi and F. R. Kschischang, “ Information transmission using the nonlinear fourier transform, part I-III,” IEEE Transactions on Information Theory, 2014.

[6] V. Aref, “Control and detection of discrete spectral amplitudes in nonlinear fourier spectrum,” arXiv preprint:1605.06328, 2016